

Electrodeposition of Zn–Co alloy coatings from sulfate–chloride electrolytes

I. KIRILOVA, I. IVANOV, St. RASHKOV†

Institute of Physical Chemistry, Bulgarian Academy of Sciences, Sofia 1113, Bulgaria

Received 12 November 1996; revised 10 April 1997

The composition, surface morphology and appearance of Zn–Co alloy deposits as a function of current density, electrode potential and Co^{2+} concentration in the electrolyte was studied. It was found that coatings of good quality with low (1%) Co content are formed at a current density of 0.2 A dm^{-2} and with high (6.5%) Co content at 2 A dm^{-2} from electrolytes containing 1.0 M Co^{2+} under galvanostatic conditions. The potentiodynamic dissolution of coatings with Co content of 6.5% indicates successive deposition of Co enriched phases and a pure Zn phase. The Zn–Co alloys are more corrosion resistant than zinc but are less resistant than cobalt.

Keywords: *corrosion resistance, electrodeposition, sulfate–chloride electrolyte, Zn–Co alloy*

1. Introduction

During the last two decades efforts to improve the corrosion stability of pure zinc coatings have been directed towards alloying it with more noble metals such as cobalt. Coatings with low Co content are less noble than steel so that they represent a sacrificial type of coating. Those with high Co content are more noble than steel and provide a barrier type of protection.

The weakly acidic electrolytes for Zn–Co alloy deposition are characterized by a current efficiency higher than 97%. Since cobalt is a more noble metal than zinc, it would be expected to deposit preferentially. However, a more complex deposition mechanism is observed. Brenner [1] has classified the codeposition of Zn and Co as anomalous because there is a prevailing deposition of the less noble metal. This prevailing Zn deposition depends on the conditions of electrodeposition, such as Zn^{2+} concentration, current density and deposition potential. Higashi *et al.* [2] have studied the mechanism of Zn alloy electrodeposition in an acidic medium containing CoSO_4 and showed that a current density exists at which Co deposition changes from normal to anomalous. The electrodeposition of Zn proceeds with initial formation of Zn(OH)_2 through which Co^{2+} discharge occurs. Therefore, Co deposition is inhibited by the stable hydroxide film. Yunus *et al.* [3] have reported that there is a change in the behaviour at the critical value of the $\text{Zn}^{2+}/\text{Co}^{2+}$ ratio. Alcalá *et al.* [4] have established that in the i/t curves for deposition on glassy carbon occurring at a variable $\text{Zn}^{2+}/\text{Co}^{2+}$ ratio and under different conditions (potential, current density, deposition time), a monotonic current increase is observed, followed by a

sharp rise, depending both on the potential applied and on the $\text{Zn}^{2+}/\text{Co}^{2+}$ ratio in the solution. At low ratios the inhibition ceased after a certain time, when a simultaneous deposition of both metals was observed which can be understood as normal. For high ratios the current increase was more gradual. A direct dependence between the i/t curve type and the coating morphology and composition was found. In the initial Zn–Co crystallites the Zn content was high, this being related to the monotonic increase in current, while the appearance of Co-enriched coatings was related to its sharp increase. The authors indicated that when the $\text{Zn}^{2+}/\text{Co}^{2+}$ ratio is higher than 1/9 and the values of the overvoltages are low, homogeneous and compact coatings, enriched with Zn are obtained. When high overvoltages were employed and/or when the $\text{Zn}^{2+}/\text{Co}^{2+}$ ratio in the solution was lower than 1/9, the Co-enriched coatings were dendritic and non-homogeneous. Gomez *et al.* [5] have studied the initial stages of Zn–Co alloy deposition at low $\text{Zn}^{2+}/\text{Co}^{2+}$ ratios (1/9) on a highly oriented pyrographite electrode. They found that the electrochemical behaviour is similar to that observed for deposits on glassy electrodes. The potentiostatic deposition begins through the formation of randomly distributed Zn-rich nuclei on the surface. When longer deposition times were used, an initial dendritic growth was observed which was related to the deposition of pure Co. Other authors [6–9] attributed the anomalous codeposition to the difference in the exchange current density between these metals.

It has been established that, with the increase in bath Co^{2+} concentration current density and temperature, Co content in the coating increases. With the increase in current density, the cathodic current efficiency decreases continuously [10–12]. The effect of H_3BO_3 on the morphology and composition of Co–Zn alloys has been studied by Karwas and Hepel

† Deceased.

[13]. The results obtained indicate that addition of H_3BO_3 in the electrolyte increases the density of nucleation in the coatings, as well as the Zn content and current efficiency. These effects are due to the adsorption of H_3BO_3 on the electrolyte surface.

This study is aimed at estimating the influence of the above-mentioned factors (current density, electrode potential and Co^{2+} concentration) on the properties of electrodeposited Zn–Co alloys.

2. Experimental details

The studies were performed in a conventional glass cell. The cathode was a 1.0 cm^2 copper plate, and both anodes were 4.0 cm^2 total surface platinum plates. Before electrolysis the cathode surface was polished with emery paper (grit 600) and etched in HNO_3 1 : 1.

The potential of the cathode was measured against a mercury sulfate reference electrode (SSE) of potential $+0.670\text{ V}$ vs NHE. The potentiostatic and potentiodynamic experiments were carried out using a potentiostat EP20 'Elpan' and scanner EG20 'Elpan'. The current–voltage curves were recorded on an X–Y plotter 'Endim 622.01'. The potential was measured with a digital voltmeter V 542.1. The galvanostatic experiments were carried out using a galvanostat 'TEC 88' and the current was measured by an ammeter ML-10.

The zinc electrolyte contained 175 g dm^{-3} $\text{ZnSO}_4 \cdot 7\text{H}_2\text{O}$, 22 g dm^{-3} $(\text{NH}_4)_2\text{SO}_4$ and 45 g dm^{-3} H_3BO_3 . Added to it were $\text{CoSO}_4 \cdot 7\text{H}_2\text{O}$ (126 g dm^{-3} , 198 g dm^{-3} and 258.5 g dm^{-3}) and $\text{CoCl}_2 \cdot 6\text{H}_2\text{O}$ (8.8 g dm^{-3} , 13.8 g dm^{-3} and 18.0 g dm^{-3}) to achieve concentrations of Co^{2+} 0.50, 0.75 and 1.00 M, respectively. As additives for deposition of bright Zn–Co alloy coatings $50\text{ cm}^3\text{ dm}^{-3}$ AZ-1 [14] (composed of ethoxylated alcohol with a general formula $\text{R}-\text{O}-(\text{CH}_2\text{CH}_2\text{O})_n\text{H}$, where R is alkyl or alkylaryl radical with 1 to 20 carbon atoms in the alkyl group and n is from 3 to 30 and of sodium or potassium salt of benzoic acid), $10\text{ cm}^3\text{ dm}^{-3}$ AZ-2 [14] (composed of benzylidene acetone and ethanol), 2 g dm^{-3} saccharin, 2 mg dm^{-3} EFAP (Na-decylsulfate) and $5\text{ cm}^3\text{ dm}^{-3}$ 30% solution of EAA (hydroxyethylated-butyn-2-diol-1,4) were used. The pH of the bath was 2.5.

Electrodeposition was performed at room temperature without stirring of the electrolyte. The anodic dissolution of the coatings was carried out potentiodynamically at a scanning rate of 10^{-3} V s^{-1} in the zinc electrolyte without additives.

The electrochemically deposited alloys were characterized by SEM, X-ray diffraction and microprobe technique.

3. Results

3.1. Zn–Co alloy composition

Figure 1 shows the dependence of Co content in the Zn–Co alloy on the current density during deposition

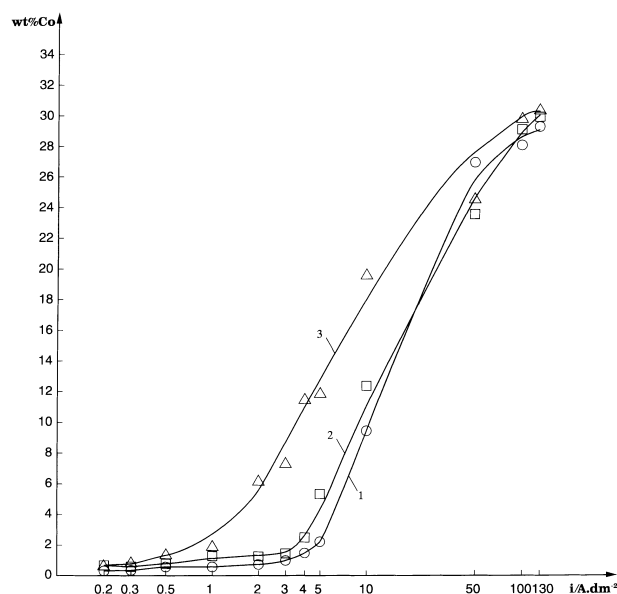


Fig. 1. Co content [wt %] in the Zn–Co alloy against current density (A dm^{-2}) during deposition in the electrolyte containing, Co^{2+} : (1) 0.50, (2) 0.75 and (3) 1.00 M.

onto a copper cathode from electrolytes containing 0.50, 0.75 and 1.00 M Co^{2+} , curves 1, 2 and 3, respectively. Three zones are distinguished on the curves: a zone of low Co content, a transition zone and a zone of high Co content. At 0.50 M Co^{2+} concentration the first zone extends to a current density of 5 A dm^{-2} and the Co content in the alloy slowly increases from 0.5 wt % (at 0.2 A dm^{-2}) to 2.5 wt % (at 5 A dm^{-2}). Within the transition zone the Co content sharply increases from 2.5 wt % (at 5 A dm^{-2}) to 27 wt % (at 50 A dm^{-2}). In the third zone (from 50 to 130 A dm^{-2}) it increases slowly from 27 to 29.5 wt %. At higher Co^{2+} concentrations, the upper limit of the first zone shifts to lower current densities (4 A dm^{-2} at 0.75 M Co^{2+} and 1 A dm^{-2} at 1.00 M Co^{2+}). In the transition zone the increase in Co content in the alloy at higher current densities proceeds more smoothly with increase in Co^{2+} concentration (curve 3). The third zone does not change significantly with increase in Co^{2+} concentration in the electrolyte.

Within the range of current densities $2\text{--}10\text{ A dm}^{-2}$ the increase in Co^{2+} concentration from 0.50 to 1.00 M causes an abrupt increase in Co content of the alloy (from 1.0 to 6.5 wt % at $i = 2\text{ A dm}^{-2}$ and from 9.5 to 20 wt % at $i = 10\text{ A dm}^{-2}$).

Figure 2 shows the dependence between Co content in the Zn–Co alloy and the potential of the cathode (at 0.50 M Co^{2+} concentration in the electrolyte). The Co content in the alloy increases from $\sim 0.6\text{ wt %}$ at -1.50 V to $\sim 10.5\text{ wt %}$ at -2.20 V .

3.2. Coating appearance and surface morphology

Table 1 presents the change in Co content, and surface appearance of the Zn–Co alloy with current density when deposition is carried out galvanostatically in electrolytes with 0.50, 0.75 and 1.00 M

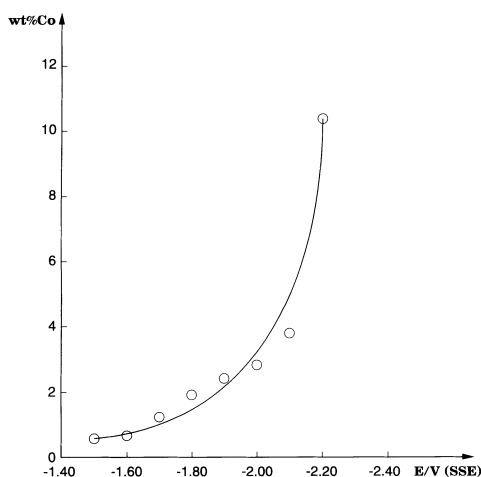


Fig. 2. Co content (wt%) in the Zn-Co alloy against cathode potential [V vs SSE] during deposition in the electrolyte containing 0.50 M Co^{2+} .

Co^{2+} concentrations. The SEM photographs in Fig. 3 illustrate the most characteristic results, shown in Table 1.

The X-ray diffraction analysis of coatings formed at 0.2 and 2 A dm^{-2} shows the presence of only the peaks, typical for Zn that correspond to $[10\bar{1}0]$ and $[11\bar{2}0]$ orientations. When the Co^{2+} concentration in the electrolyte is 0.50 M, the $[11\bar{2}0]$ orientation is much more pronounced as compared to $[10\bar{1}0]$. The reverse case is observed for the other two concentrations (0.75 and 1.00 M) though the difference is small.

Table 2 shows the change in Co content and surface appearance of Zn-Co alloy coating as a function of cathodic potential when deposition is carried out potentiostatically in electrolyte containing 0.5 M Co^{2+} .

3.3. Anodic dissolution of Zn-Co alloy coatings

Figure 4 shows the anodic curves of the dissolution of 0.3 μm thick Zn, Co and Zn-Co alloy coatings. It is seen that during the dissolution of the Zn coating (deposited at current density of 2 A dm^{-2} from an

electrolyte containing only Zn^{2+}), curve 1, a peak appears on the current-voltage curve at a potential -1.300 V. It is three times higher than the second peak at -1.240 V. On the anodic polarization curve (curve 2), obtained during the dissolution of the Co coating (deposited at 2 A dm^{-2} from an electrolyte containing only Co^{2+}), a peak appears at a potential -0.640 V with a weakly expressed inflexion at -0.625 V. During the dissolution of the Zn-Co(1%) coating, obtained at 0.2 A dm^{-2} from an electrolyte containing both Zn^{2+} and Co^{2+} , only one peak appears on the voltammogram at -1.305 V. Due to the low Co content (1%), the corresponding dissolution peak is very small and cannot be observed on the curve at this scale. When dissolving anodically a Zn-Co(6.5%) alloy coating, deposited at 2 A dm^{-2} from an electrolyte containing both Zn^{2+} and Co^{2+} , three peaks appear (curve 4). The highest is the one at potential -1.280 V, the lower is at -1.125 V and the lowest is at -0.900 V.

Figure 5 shows the dissolution curves of 3.0 μm thick coatings. The dissolution peak of the Zn coating, deposited at 2 A dm^{-2} from a Zn^{2+} containing electrolyte (curve 1), is at a potential -1.210 V, while that one of the Co coating, obtained at the same current density but from a Co^{2+} containing electrolyte, is at -0.525 V. When a coating with low Co content, deposited at 0.2 A dm^{-2} from an electrolyte containing Zn^{2+} and Co^{2+} , is dissolved (curve 3), a peak at -1.150 V appears, which is due to Zn dissolution. However, the peak typical for Co dissolution is not observed on the curve. When a coating with high Co content (6.5%), obtained at 2 A dm^{-2} , is dissolved, the voltammogram (curve 4) shows a high peak at -1.200 V with an inflexion at -1.075 V and a smaller one at -0.900 V.

4. Discussion

Figure 1 indicates that increasing the Co^{2+} concentration in the zinc electrolyte to 1.00 M enables the

Table 1. Appearance of the coatings obtained in zinc electrolytes containing 0.50, 0.75 and 1.00 M Co^{2+} as a function of the current density

$i/\text{A dm}^{-2}$	Co^{2+}		
	0.50 M	0.75 M	1.00 M
130	29.44% dark, spongy, friable	30.18% dark, spongy, friable	30.67% dark, spongy, friable
100	28.24% dark, spongy, friable	29.37% dark, spongy, friable	30.14% dark, spongy, friable
50	27.12% dark, spongy friable	23.84% dark, spongy, friable	24.92% dark, spongy friable
10	9.66% dark and light areas	12.68% dark and smooth, spongy at places	20.00% dark, spongy
5	2.42% dark, burnt out at edges, bright in the middle	5.64% dark, spongy at the edges	12.27% smooth, dark
4	1.68% dark	2.80% non-homogeneous with island structure	11.90% smooth, dark
3	1.18% smooth, bright	1.75% homogeneous with dark spots	7.73% succeeding bright and dark grey areas
2	0.93% smooth, bright	1.56% bright, dark at the edges	6.59% smooth, bright
1	0.76% smooth, bright	1.57% smooth, bright	2.30% smooth, bright
0.5	0.76% smooth, bright	1.07% smooth, bright	1.76% smooth, bright
0.3	0.54% smooth, bright	0.88% smooth, bright	1.20% smooth, bright
0.2	0.50% smooth, bright	0.96% smooth, bright	1.00% smooth, bright

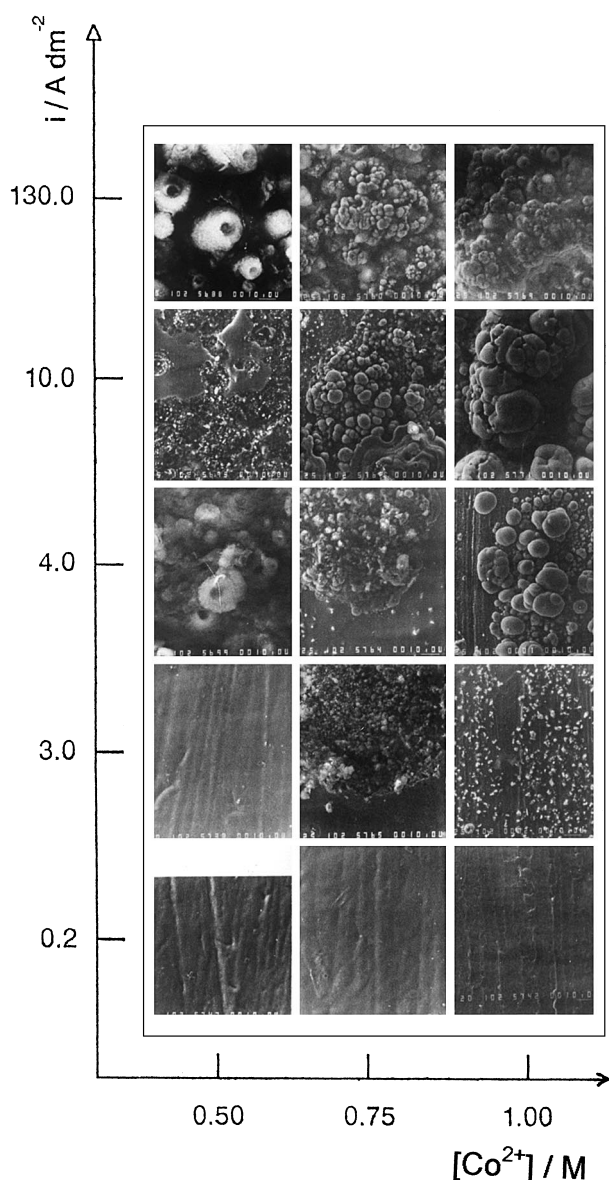


Fig. 3. Scanning electron micrographs showing the surface morphology of Zn-Co alloy coatings obtained at different current densities and Co^{2+} concentration in the electrolyte. Magnification $\times 1320$.

deposition of alloy coatings with high Co content at comparatively low current densities (from 2 to 5 A dm^{-2}). Fig. 2 shows that under potentiostatic conditions, coatings with low Co content (0.6–

Table 2. Appearance of the coatings obtained in zinc electrolytes containing 0.50 M Co^{2+} as a function of the cathode potential

E/V vs SSE	$\text{Co}^{2+} = 0.50 \text{ M}$
-2.20	10.38% spongy at the edges, dark in the middle, friable
-2.10	3.80% dark, smooth, burnt out
-2.00	2.83% succeeding dark and light areas
-1.90	2.42% bright in the middle, dark at the edges
-1.80	1.92% smooth, bright
-1.70	1.23% smooth, bright
-1.60	0.66% smooth, bright
-1.50	0.57% smooth, bright

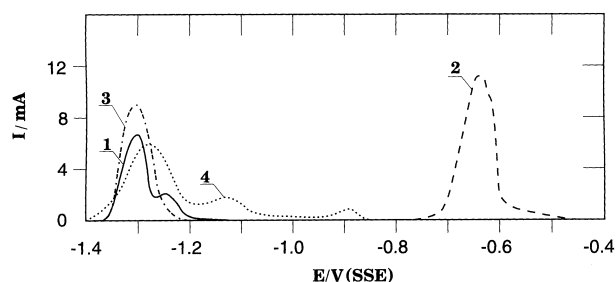


Fig. 4. Current-voltage curves of the dissolution of (1) Zn coating obtained at 2 A dm^{-2} , (2) Co coating obtained at 2 A dm^{-2} , (3) Zn-Co(1%) alloy obtaining at 0.2 A dm^{-2} from zinc electrolyte containing 1 M Co^{2+} and (4) Zn-Co(6.5%) alloy obtaining at 2 A dm^{-2} from zinc electrolyte containing 1 M Co^{2+} . Coating thicknesses $0.3 \mu\text{m}$. Scan rate 10^{-3} V s^{-1} .

0.7 wt %) are deposited at potentials from -1.50 to -1.60 V , while those with high Co content are deposited at -2.20 V .

From Table 1 and Fig. 3 it is seen that the most homogeneous, smooth, bright (or semibright) coatings (with a good adhesion to the substrate) are deposited from the electrolyte containing 1 M Co^{2+} : with low (1%) Co content at a current density from 0.2 to 0.3 A dm^{-2} , or with high (6.5%) Co content at a current density from 2 to 3 A dm^{-2} . At high current densities the coatings formed are dark, spongy and friable, though the content of Co is 2–3 times higher.

From Table 2 it is seen that the coatings are smooth and bright when deposited at potentials from -1.50 to -1.80 V . At more negative potentials the coatings obtained are dark, spongy and friable. At the same time the Co content in all cases is relatively lower than for galvanostatic deposition.

The existence of three peaks on the anodic voltammograms (Figs 4 and 5, curves 4) reveals that the

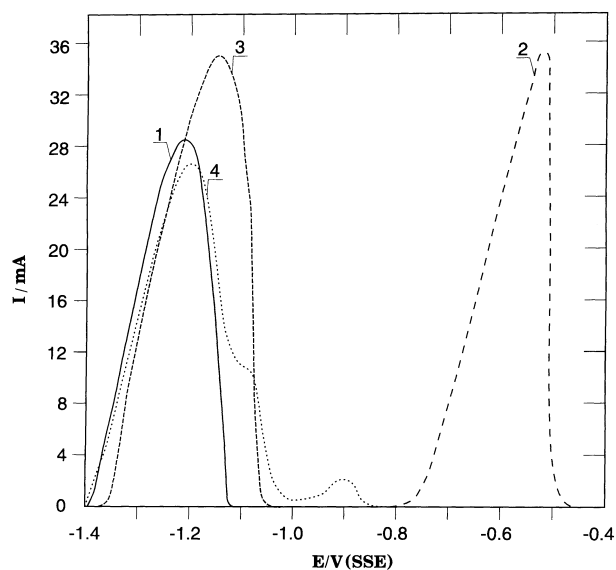


Fig. 5. Current-voltage curves of the dissolution of (1) Zn coating obtained at 2 A dm^{-2} , (2) Co coating obtained at 2 A dm^{-2} , (3) Zn-Co(1%) alloy obtaining at 0.2 A dm^{-2} from zinc electrolyte containing 1 M Co^{2+} and (4) Zn-Co(6.5%) alloy obtaining at 2 A dm^{-2} from zinc electrolyte containing 1 M Co^{2+} . Coating thicknesses $3.0 \mu\text{m}$. Scan rate 10^{-3} V s^{-1} .

coatings contain not only Zn (the highest peaks) but also Zn–Co alloy of different content and structure (the two lower peaks on both curves 4). These curves indicate that simultaneously with the basic Zn depositions, smaller quantities of a Zn–Co alloy are deposited. The alloy is more corrosion resistant than Zn but is less resistant than Co.

5. Conclusions

The deposition of Zn–Co alloys is most successfully carried out from an electrolyte containing 1.0 M Co^{2+} under galvanostatic conditions. Coatings of good quality with low Co content are deposited at a current density of 0.2 A dm^{-2} , while those of high Co content are deposited at 2 A dm^{-2} .

The potentiodynamic dissolution of coatings deposited galvanostatically from an electrolyte containing Zn^{2+} and Co^{2+} with high (6.5%) Co content indicates a successive deposition of Co-enriched phases and a pure Zn phase. At low (1%) Co content in the coating the existence of Co-enriched phases cannot be established.

The Zn–Co alloys are more corrosion resistant than zinc but is less resistant than cobalt.

Acknowledgements

The authors highly appreciate the financial assistance provided by the National Foundation 'Scientific Investigations', Bulgaria.

References

- [1] A. Brenner, 'Electrodeposition of Alloys, Principles and Practice', Academic Press, New York (1963).
- [2] K. Higashi, H. Fukushima and T. Urakava, *J. Electrochem. Soc.* **128** (1981) 2081.
- [3] M. Yunus, C. Capel-Boute and C. Decroly, *Electrochim. Acta* **10** (1965) 885.
- [4] M. Alcala, E. Gomez and E. Valles, *J. Electroanal. Chem.* **370** (1994) 73.
- [5] E. Gomez, E. Valles, P. Gorostiza, J. Servat and F. Sanz, *J. Electrochem. Soc.* **142** (1995) 4091.
- [6] M. Mathias and T. Chapman, *ibid.* **134** (1987) 1408.
- [7] M. Mathias and T. Chapman, *ibid.* **137** (1990) 102.
- [8] R. Fratesi and G. Roventi, *Mater. Chem. Phys.* **23** (1989) 529.
- [9] D. Landolt, *Electrochim. Acta* **39** (1994) 1075.
- [10] W. Verberne, *Trans. Inst. Met. Finish.* **64** (1969) 30.
- [11] A. Shears, *Trans. Inst. Met. Finish.* **67** (1989) 67.
- [12] J. Zhang, Z. Yang, M. An, W. Li and Z. Tu, *Plat. Surf. Fin.* **82** (1995) 135.
- [13] C. Karwas and T. Hepel, *J. Electrochem. Soc.* **136** (1989) 1672.
- [14] Bulgarian Patent *N 39 402* (1978), *N 27 305* (1979).